First measurement of the scrape-off layer current profile using electron directional probe on W7-X with an island divertor configuration

L. Liao[1,2,3], Y. Liang[1], A. Knieps[1], P. Drews[1], S.C. Liu[2], C. Killer[4], J. Yang[1,5], D. Cipciar[4], D. Nicolai[1], O. Neubauer[1], G. Satheeswaran[1] and the W7-X Team

[1] *Forschungszentrum Jülich GmbH, Institut für Energie- und Klimaforschung – Plasmaphysik, 52425 Jülich, Germany*

[2] *Institute of Plasma Physics, Chinese Academy of Sciences, Hefei 230031, China*

[3] *University of Science and Technology of China, Hefei, 230026, China*

[4] *Max Planck Institute for Plasma Physics, 17491 Greifswald, Germany*

[5] *Huazhong University of Science and Technology, Wuhan, Hubei 430074, China*

1. Motivation

W7-X, as a stellarator, unlike tokamaks, builds its magnetic field pure by external coils. The magnetic topology, especially magnetic islands and stochastication of the magnetic field in the edge, largely affects the scrape-off layer (SOL) profiles, plasma turbulence behaviour, dynamic and transport. Thus, the determination of magnetic topology is worth investigating.

In the plasma, due to its to smaller mass, the velocity of an electron is 43 times faster than a proton, i.e. the Larmor radius of an electron is 1/43 of the Larmor radius of a proton, if they share the same energy. That makes electrons a better indicator of magnetic topology than ions.

Since the current equals the product of particle density, electric charge and its velocity, the current in the plasma is mostly contribute by electrons. If direct measurement of edge plasma current profile is proposed, that is electron current measurement.

2. Experimental set up

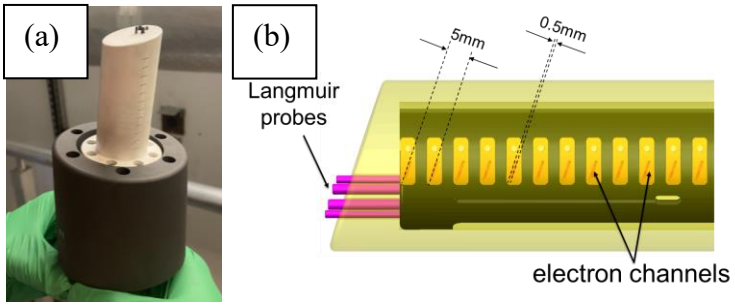

Fig.1: (a) Actual DEP probe head, (b) Side view of the DEP

A novel method called directional electron probe (DEP) is introduced for the purpose of measuring the current distribution in the edge. It composed of two opposing channels, as shown in Fig. 1, with their connecting line aligning with the local magnetic field line. Each channel

features a narrow radial aperture and sufficient thickness to obstruct high-energy ions, owing to their large Larmor radii. At the termination of the aperture, the collector is positively biased to repel low-energy ions. Consequently, the dominant contributor to the collected current of DEP is electrons.

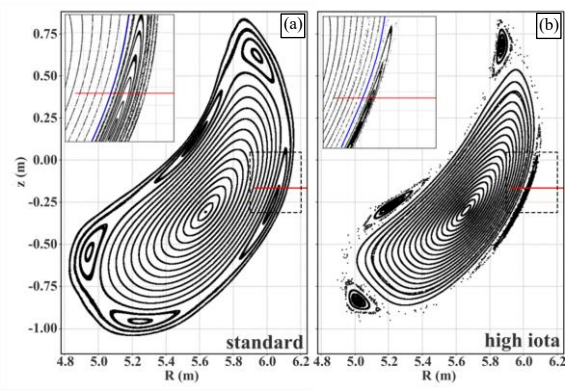

Fig. 2: Poincare plots of W7-X (a) standard configuration (b) high iota configuration, probe path is indicated in red

The path of the MPM with respect to the magnetic topology is indicated in the Poincare plots in figure 2 for two representative magnetic configurations. In the magnetic standard configuration (Fig. 2(a)), the MPM crosses the 5/5 island chain about 10 cm above the island's O-point. In the high iota configuration (Fig. 2(b)), in contrast, the MPM again crosses slightly above the O-point of a very narrowly compressed island. The connection length in high-iota configuration is much shorter compared with standard configuration.

3. Results

The scrape-off layer current profile in high iota configuration

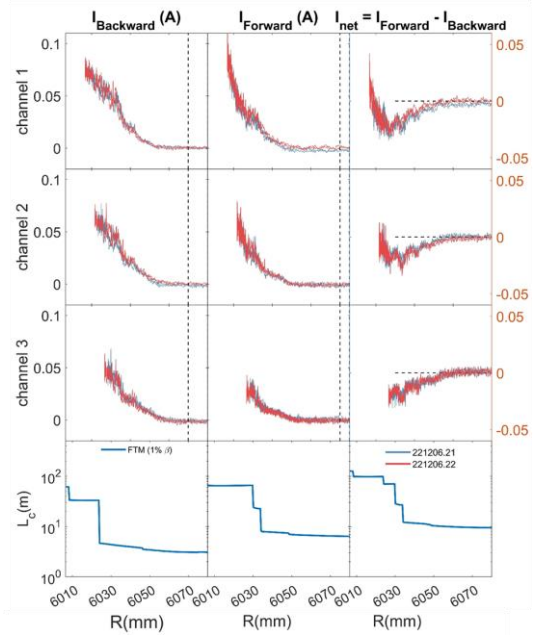

Fig. 4: Current profile in the probe path of high iota configuration (First three channels)

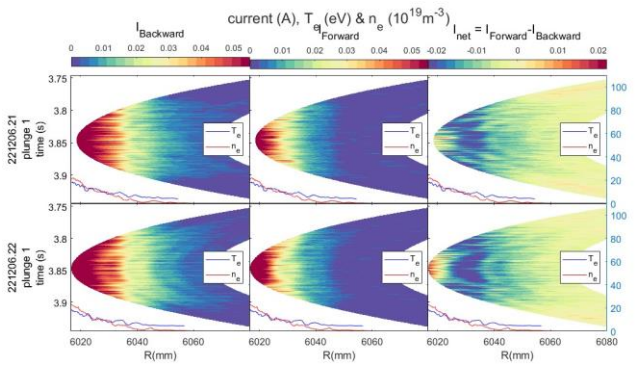

Fig. 3: T_e, n_e profile and current evolution of high iota configuration during the plunge

In high iota configuration, stable current profile is shown in the fig of two shots showing a stable current profile during the whole plunge

process. In the low connection region, measured $I_{net} < 0$. Current reversal (change in direction of current) was found at R = 6020 mm.

The scrape-off layer current profile in standard configuration

———— with & without Control Coils (CC)

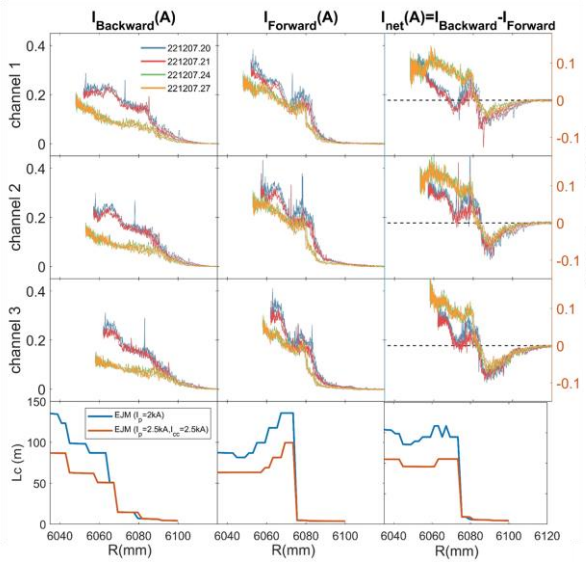

Fig. 6: Current profile in the probe path of standard configuration (First three channels)

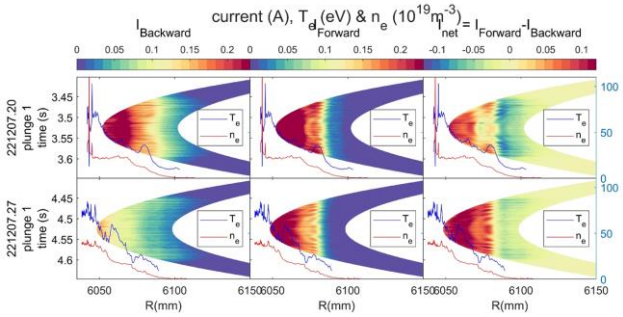

Fig. 5: T_e, n_e profile and current evolution of standard configuration during the plunge

In the standard configuration, four shots with different plasma current and control coils settings are shown in the fig. The result in respective settings are in good repeatability and high consistency, showing a stable current profile with time events during plunges. Features in current profile are related to connection length profile (e.g. gradual climb of $I_{Backward}$ from R = 6100mm and sudden increase of at around R = 6080 mm). Maximum J_{net} measured was beyond 20 A/cm^2.

4. Summary and outlooks

The SOL current profile has been measured in the scrape-off layer of W7-X in both high-iota and standard configuration. Stable current profiles of distinguish spatial structure exist in each configuration which are determined by magnetic topology. Comprehensively, the direction and the amplitude of directional current in the SOL region is decided by local n_e, T_e and interaction with target. Also, edge current profile modification is clearly observed when changing magnetic topology through the control of Control Coils.

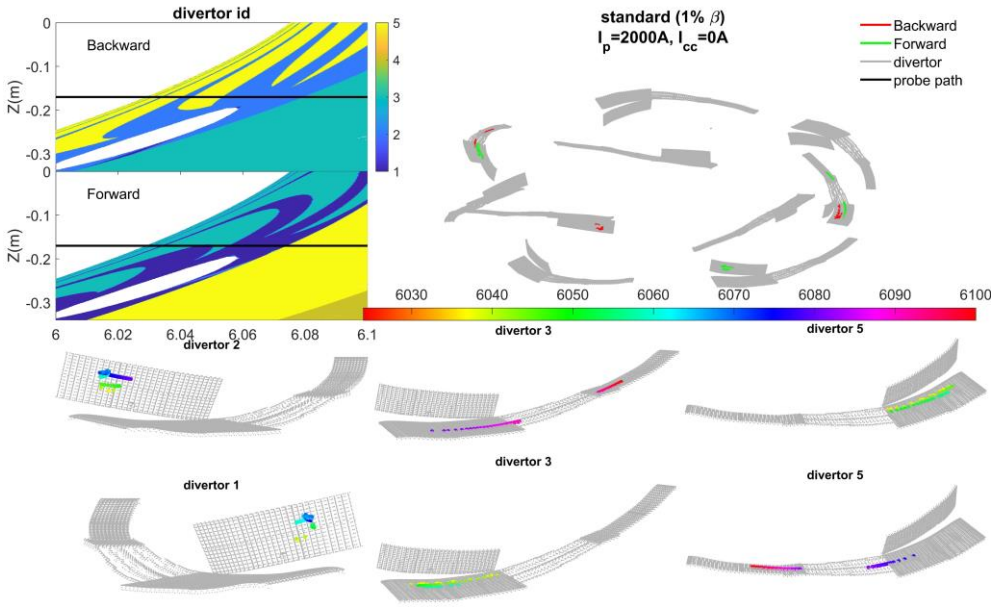

Fig.7 Map of divertor targets intersecting the field lines

Predicted by Peter C. Stangeby, thermoelectric effect is thought to be responsible for the formation of the measured current [5]. Simulation and experiment have also been carried out for promotion and validation [6][7]. Fig 5 shows the map of divertor targets intersecting the filed lines in standard configuration with 2000A plasma current. 2D or 3D current extrapolation could be achieved later after successful validation between Space-Charge Limited Current model, W7-X experiment data and modeling results.

5. Acknowledgment

This work has been carried out within the framework of the EUROfusion Consortium, funded by the European Union via the Euratom Research and Training Programme (Grant Agreement No 101052200 — EUROfusion). Views and opinions expressed are however those of the author(s) only and do not necessarily reflect those of the European Union or the European Commission. Neither the European Union nor the European Commission can be held responsible for them.

6. Reference

[1] S.C. Liu et al., Nuclear Materials and Energy 29 101080 (2021)

[2] S.C. Liu et al Nuclear Fusion 61 126004 (2021)

[3] Liang Y, et al. Nuclear Fusion 57 066049 (2017)

[4] C. Killer et al Nuclear Fusion 59 086013 (2019)

[5] Peter C Stangeby, The plasma boundary of magnetic fusion device (2000).

[6] S. Takamura, Contrib. Plasma Phys.44, No. 1-3, 126 – 137 (2004)

[7] M. Komm et al, Nuclear Fusion 60 054002 (2020)